THE JOURNAL OF BIOLOGICAL CHEMISTRY
Vol. 277, No. 36, Issue of September 6, pp. 33284–33290, 2002

Printed in U.S.A.

Oxidant-induced Vascular Endothelial Growth Factor Expression in Human Keratinocytes and Cutaneous Wound Healing*

Received for publication, April 9, 2002, and in revised form, June 11, 2002
Published, JBC Papers in Press, June 14, 2002, DOI 10.1074/jbc.M203391200

Chandan K. Sen‡§, Savita Khanna‡, Bernard M. Babior¶, Thomas K. Hunt‡, E. Christopher Ellison‡, and Sashwati Roy‡

From the ‡Laboratory of Molecular Medicine, Dorothy M. Davis Heart and Lung Research Institute, Department of Surgery (Center for Minimally Invasive Surgery), The Ohio State University Medical Center, Columbus, Ohio 43210 and the ¶Department of Molecular and Experimental Medicine, Division of Biochemistry, The Scripps Research Institute, La Jolla, California 92037

Neutrophils and macrophages, recruited to the wound site, release reactive oxygen species by respiratory burst. It is commonly understood that oxidants serve mainly to kill bacteria and prevent wound infection. We tested the hypothesis that oxidants generated at the wound site promote dermal wound repair. We observed that H_2O_2 potently induces vascular endothelial growth factor (VEGF) expression in human keratinocytes. Deletion mutant studies with a VEGF promoter construct revealed that a GC-rich sequence from bp −194 to −50 of the VEGF promoter is responsible for the H_2O_2 response. It was established that at μM concentrations oxidant induces VEGF expression and that oxidant-induced VEGF expression is independent of hypoxia-inducible factor (HIF)-1 and dependent on Sp1 activation. To test the effect of NADPH oxidase-generated reactive oxygen species on wound healing *in vivo*, Rac1 gene transfer was performed to dermal excisional wounds left to heal by secondary intention. Rac1 gene transfer accelerated wound contraction and closure. Rac1 overexpression was associated with higher VEGF expression both *in vivo* as well in human keratinocytes. Interestingly, Rac1 gene therapy was associated with a more well defined hyperproliferative epithelial region, higher cell density, enhanced deposition of connective tissue, and improved histological architecture. Overall, the histological data indicated that Rac1 might be an important stimulator of various aspects of the repair process, eventually enhancing the wound-healing process as a whole. Taken together, the results of this study indicate that wound healing is subject to redox control.

Wound healing commences with blood coagulation followed by infiltration of neutrophils and macrophages at the wound site to release reactive oxygen species (ROS)[1] by an oxygen-consuming respiratory burst. It is commonly understood that oxidants serve mainly to kill bacteria and prevent wound infection (1). Recent studies show that at low concentrations ROS may serve as signaling messengers in the cell and regulate numerous signal transduction and gene expression processes (2–5). Previous studies from our laboratories have reported that in the wound site ROS may promote wound angiogenesis by inducing VEGF expression in wound-related cells such as keratinocytes and macrophages (6–8). Specifics of the signaling path involved in ROS-induced VEGF expression remain unknown, however.

The Rac GTPase belongs to the rho family of small GTP binding proteins, and its role in the production of ROS in phagocytic cells such as neutrophils is well established (9). Rac proteins are essential for the assembly of the plasma membrane NADPH oxidase that is responsible for the transfer of electrons to molecular oxygen leading to the production of superoxide anions during respiratory burst. Rac proteins, in particular Rac1, serve a similar function in nonphagocytic cells (10, 11). Rac1 regulates cell growth, migration, and cellular transformation by increasing the intracellular production of ROS (10, 12–14). The objectives of the current study were 2-fold. First, characterize the transcriptional control of H_2O_2-inducible VEGF expression in human keratinocytes. Second, we sought to examine whether Rac1 overexpression influences inducible VEGF expression in keratinocytes. To test the hypothesis that ROS promotes wound repair, a murine secondary-intention wound-healing model was employed to investigate whether Rac1 gene transfer regulates wound contraction and closure.

EXPERIMENTAL PROCEDURES

Materials and Plasmids

Herbimycin, geldanamycin, and lavendustin A were obtained from Calbiochem, San Diego, CA. Recombinant human tumor necrosis factor-α (TNFα) and VEGF ELISA kits were from R&D Systems, Minneapolis, MN. Diphenyleneiodonium (DPI), mithramycin, H_2O_2, and unless otherwise stated, all other chemicals were obtained from Sigma.

The empty plasmid pEXV and the expression plasmid pEXVracV12 (encoding Myc epitope-tagged constitutively active Rac1) were provided by Dr. K. Irani (10). SP-1 Luc, where three repeat SP1 consensus sites are placed upstream of a luciferase gene, was provided by Dr. P. Farnham (15). The VEGF reporter constructs (see Fig. 3), containing sequences derived from the human VEGF promoter-driving expression of the firefly luciferase gene, were provided by Dr. D. Mukhopadhyay. The deletion mutant constructs, derived from the 2.6-kb VEGF promoter fragment using polymerase chain reaction, were subcloned into pGL-2 basic vector (Promega) as described (16).

Cells and Cell Culture

Immortalized human keratinocytes line HaCaT (17) were grown as described (6, 7). Adult human epidermal keratinocytes were obtained from Cascade Biologics Inc. (Portland, OR) and grown as described (6). VEGF protein expression by keratinocytes was determined using an ELISA approach described previously (6, 7).

* Supported by National Institutes of Health Grant GM 27345 (to C. K. S.). The costs of publication of this article were defrayed in part by the payment of page charges. This article must therefore be hereby marked "*advertisement*" in accordance with 18 U.S.C. Section 1734 solely to indicate this fact.

§ To whom correspondence should be addressed: 512 Heart and Lung Research Inst., 473 W. 12th Ave., Columbus, OH 43210. Tel.: 614-247-7786; Fax; 614-247-7818; E-mail: sen-1@medctr.osu.edu.

[1] The abbreviations used are: ROS, reactive oxygen species; HIF, hypoxia-inducible factor; VEGF, vascular endothelial growth factor; ELISA, enzyme-linked immunosorbent assay; DPI, diphenyleneiodonium; HPLC, high pressure liquid chromatography; GFP, green fluorescence protein.

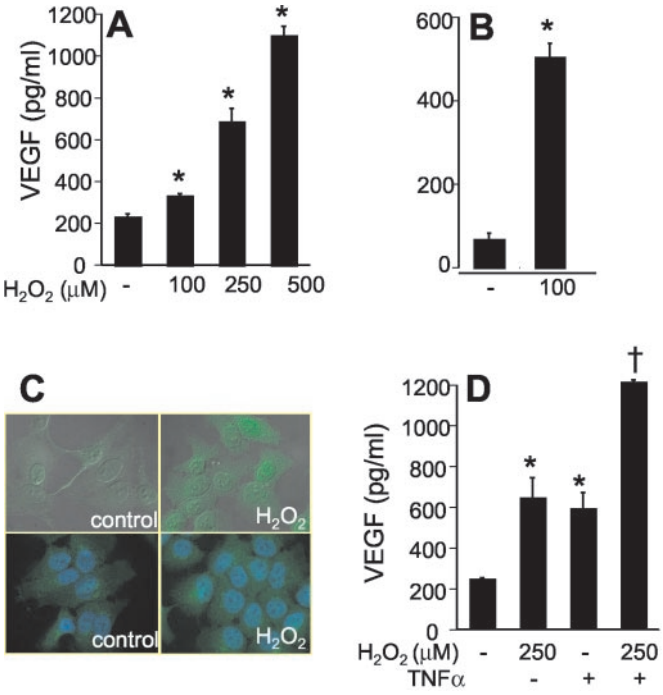

FIG. 1. **H_2O_2 induced VEGF expression in human keratinocytes.** HaCaT keratinocyte line (*A*, *C*, and *D*) or primary adult human epidermal keratinocytes (*B*) were challenged either with H_2O_2 and/or with TNFα (25 ng/ml) as indicated for 12 h. VEGF release in the media was measured by ELISA (*A*, *B*, and *D*). *C*, cells treated with H_2O_2 (250 μM, 12 h) were immunostained with anti-VEGF primary and fluorescein isothiocyanate (shown in *green*)-conjugated secondary antibody. In the *lower panels*, the nuclei were stained with 4′,6-diamidino-2-phenylindole (shown in *blue*). *, $p < 0.001$ when compared with corresponding H_2O_2 or TNFα non-treated cells. †, $p < 0.001$ when compared with cells treated with H_2O_2 or TNFα alone.

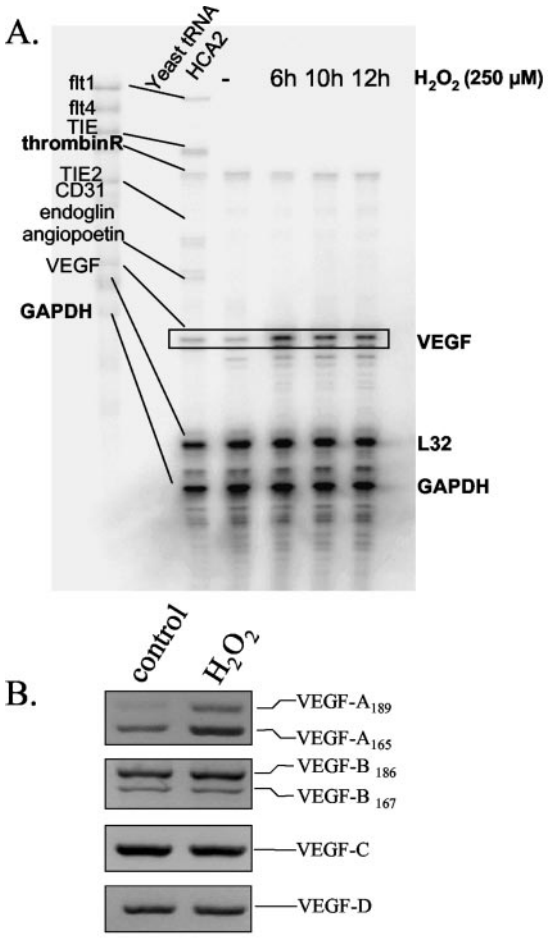

FIG. 2. **H_2O_2-sensitive gene expression related to angiogenesis.** *A*, HaCaT cells were activated with H_2O_2 for 6–12 h. RNase protection assay data shown. *B*, HaCaT cells were activated with H_2O_2 for 6 h. VEGF isoforms and its homologues (VEGF-B, -C, and -D) were detected using reverse transcription-PCR.

Immunofluorescent Staining of VEGF

HaCaT cells treated or not treated with H_2O_2 (250 μM, 12 h) were fixed in 3.7% formaldehyde solution. Cells were then permeabilized with phosphate-buffered saline containing 0.2% Triton X-100, and nonspecific antibody binding was blocked. VEGF expression was detected using anti-goat-hVEGF (1:50 dilution; R&D Systems). To enable fluorescence detection, cells were incubated with anti-goat-IgG-fluorescein isothiocyanate (Santa Cruz, San Diego, CA) secondary antibody (1:100 dilution). The nuclei were stained with 4′,6-diamidino-2-phenylindole (Molecular Probe).

RNase Protection Assay and Reverse Transcription-PCR

Total RNA was isolated from cells with Trizol reagent (Invitrogen). The mRNA were detected from total cell RNA by RNase protection assay utilizing DNA templates from BD PharMingen (BD RiboQuant™ Ribonuclease Protection Assay System, BD PharMingen, San Diego, CA) (6, 7). VEGF-A (splice variants VEGF206, VEGF189, and VEGF165), VEGF-B (splice variants VEGF-B186 and VEGF-B167), VEGF-C, and VEGF-D were detected by reverse transcription-PCR using commercially available primer pairs (R&D Systems) and previously described routine protocol (6).

Transient Transfection and Luciferase Assay

HaCaT cells were transiently transfected with the VEGF-Luc and Sp1-Luc constructs using SuperFect (Qiagen) reagent according to the manufacturer's instructions. After 18 h of transfection, the cells were activated for 4–6 h with H_2O_2. Luciferase reporter activity was determined using a commercial kit (Stratagene). To block Sp1 interaction to its specific DNA-binding sites HaCaT cells were incubated with 100 nM mithramycin (Sigma) 2 h prior to activation of the cells with H_2O_2.

Expression of Rac1 in Cells

Following 18 h of seeding, HaCaT cells were transiently transfected with either the empty expression plasmid pEXV or the expression plasmid pEXVracV12 (constitutively active Rac1) using SuperFect transfection reagent (Qiagen). The cells were maintained in regular culture condition for 24 h to allow for protein expression.

Immunoblot Analyses

For Rac1 immunoblot, cytosolic protein extract of cells transiently transfected with pEXV or pEXVRac1V12 plasmids were separated on a 10% SDS-polyacrylamide gel under reducing conditions, transferred to nitrocellulose, and probed with anti-Rac1 antibody (1:1000 dilution; Upstate Biotech, Lake Placid, NY).

Protein Phosphotyrosine

Using standard Western blot techniques we were not available to get a high-quality resolution of bands. Instead, we labeled cellular proteins with ^{35}S (18). Tyrosine-phosphorylated proteins were immunoprecipitated, and autoradiography was performed as described previously (18).

GSH/GSSG

GSH and GSSG were simultaneously detected from wound edge tissues using a HPLC-coulometric electrode array detector (Coularray Detector, model 5600 with 12 channels; ESA Inc., Chelmsford, MA). For extraction, wound edge tissues were pulverized in liquid nitrogen and then homogenized in 5% wt/v *m*-phosphoric acid using a Teflon homogenizer. The samples were snap frozen and stored in liquid nitrogen until the HPLC assay. On the day of HPLC assay, samples were quickly thawed on ice and centrifuged (12,000 × *g*, 5 min) at 4 °C. Supernatants were collected and filtered through a 0.2-μM filter. The filtrate was immediately injected to HPLC. GSH and GSSH were separated using a C18 column and the following mobile phase: 50 mM sodium dihydrogen phosphate, 0.5 mM octanosulphonic acid, and 3% acetonitrile at pH 2.7 (19). The coulometric electrode array offers several advantages over conventional single-channel detectors (20). Using a progressively increasing oxidative array of 12 electrodes, compounds can

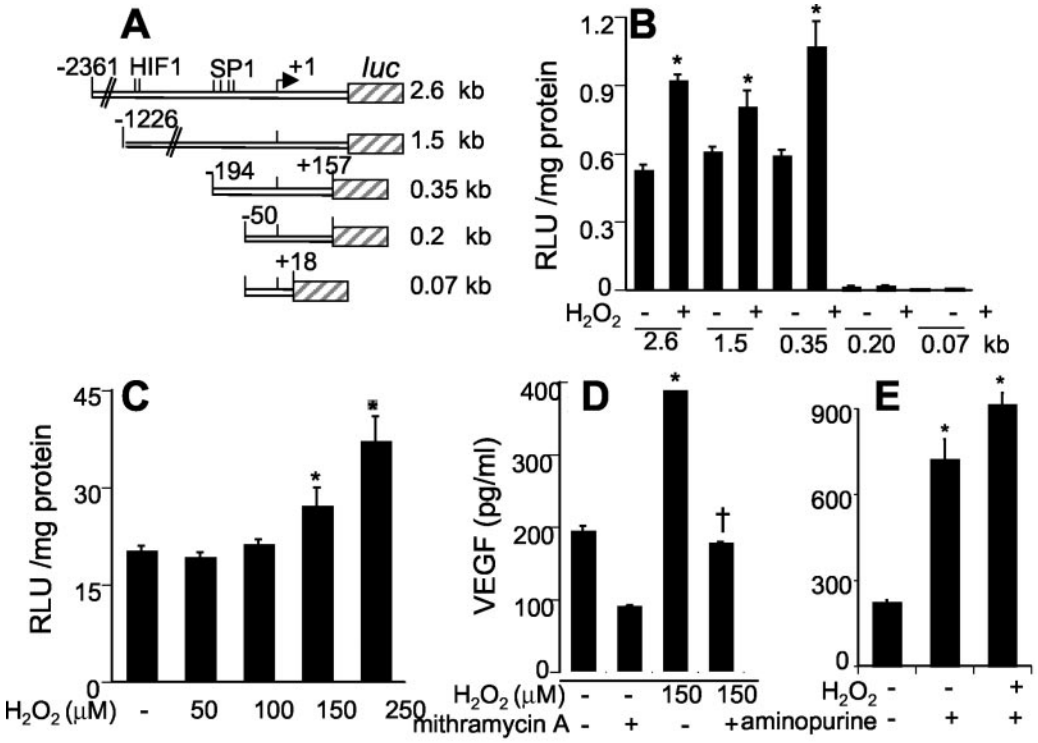

FIG. 3. **Deletion mutant construct analysis of H_2O_2-sensitive site in the VEGF promoter.** *A*, schematized VEGF promoter deletion constructs. The HIF-1 site is centered at bp −965 (41), while GC boxes reside between bp −94 and −51 (42). *B*, deletion analysis of VEGF promoter revealed a H_2O_2-responsive *cis* element from bp −194 to −50. VEGF reporter constructs were transiently transfected in HaCaT cells. After 18 h of transfection, the cells were activated for 6 h with H_2O_2 in a serum-free media. *C*, H_2O_2-induced activation of Sp1-Luc in HaCaT cells. *D*, treatment of cells with SP1-inhibitor mithramycin (100 nM) completely blocked H_2O_2-induced VEGF expression. *E*, aminopurine (1 mM), inhibitor of the HIF-1 path, did not influence H_2O_2-induced VEGF expression. VEGF expression was measured by ELISA. *, $p < 0.01$ when compared with corresponding H_2O_2 non-treated cells. †, $p < 0.001$ when compared with corresponding mithramycin-untreated cells.

be made to react at three consecutive sensors. The upstream electrode oxidizes a small portion of the analyte, the second dominant electrode oxidizes the bulk of the analyte, and the downstream electrode oxidizes the remainder. A particular standard eluting at a given retention time will always provide a predictable response across these three electrodes. The ratio of the response across these three electrodes remains constant and is referred to as ratio accuracy. The comparison of ratio accuracy of standard *versus* sample is powerful and an immediate indicator of peak purity. Compared with standard, lower ratio accuracy in sample will indicate the presence of a co-elutant.

Secondary-intention Excisional Dermal Wound Model

Male BALB/c mice ($n = 10$; 4–6 weeks of age) were used. Two 8 × 16-mm full-thickness excisional wounds (6) were placed on the dorsal skin, equidistant from the midline and adjacent to the four limbs (see Fig. 9*A*). When required, the animals were killed and cutaneous wound edges (1–1.5 mm) were harvested.

Rac1 Gene Transfer

Each of the two wounds was topically treated once daily (days 0–5) with either empty plasmid (pEXV) or expression plasmid pEXVracV12 (constitutively active Rac1) (21). Twenty-five microliters of naked plasmid DNA (10 μg) in sterile Tris-EDTA, pH 8.0, (TE) were administered onto the wound area and spread evenly using the pipette tip. The applied DNA was allowed to completely air dry on the treated skin, which took ~10 min. Plasmid amplification and purification were performed using standard procedures (22). To study the effect of Rac1 gene therapy on endothelial cell response, transgenic mice (FVB/N-TgN-TIE2GFP) were wounded ($n = 3$) as described above. This strain expresses green fluorescent protein (GFP) under the direction of the endothelial-specific receptor tyrosine kinase (Tie2) promoter. All animal protocols were approved by the Institutional Lab Animal Care and Use Committee of the Ohio State University, Columbus, OH.

Determination of Wound Area

Imaging of wounds was performed between days 0–14 of wounding using a digital camera (Mavica FD91, Sony). The wound area was determined using WoundMatrix™ software.

Collagen Content

Collagen content of wound edge tissue was assessed by determining the amount of hydroxyproline (23). Frozen wound tissue was pulverized under liquid nitrogen and then hydrolyzed in 1 ml of 5 N HCl overnight at 110 °C. The reaction was neutralized with 2.5 N NaOH. The hydroxyproline assay was done in a 96-well plate by adding 100 μl of oxidizing solution to wells. The oxidizing solution was prepared by adding 6 mg of chloramine T/ml of oxidation buffer (3 ml of isopropyl alcohol, 1.65 ml of H_2O, 1.95 ml of citrate-acetate buffer, pH 6). Next, 50 μl of standard or sample was added to each well. This was followed by addition of 100 μl of Ehrlich's reagent (6 g of *p*-dimethylaminobenzaldehyde dissolved in 52 ml of isopropyl alcohol and 16 ml of 50% perchloric acid) to each well. After incubating the samples at 60 °C for 45 min, the samples were cooled to room temperature. Absorbance was measured at 562 nm, and the amount of hydroxyproline present in samples was determined by comparison to a standard curve.

Histology

Formalin-fixed wound edges were embedded in paraffin and sectioned. The sections (4 μm) were deparaffinized and stained with the following primary antibodies: rabbit polyclonal antibodies to Rac1 (BD Transduction Laboratories), anti-VEGF (R&D Systems), or anti-tenascin (Chemi-Con International).

GFP Visualization—Freshly dissected, unfixed wound edge was snap-frozen and immediately cut into 10 μm frozen sections. GFP expression was visualized and imaged using a fluorescent microscope (Nikon E800 with MetaMorph version 4.5 software, Universal Imaging Corp.). Image of the same frame shown in Fig. 6*C* was also captured using Differential Interference Contrast (DIC, Nomarski) optics.

Masson Trichrome Staining—Wound edge sections (4 μm) were deparaffinized and stained using Masson Trichrome procedure (24). This procedure result in blue-black nuclei, blue collagen and cytoplasm, and keratin, muscle fibers, and intracellular fibers all stained red.

Statistics

In vitro data are reported as mean ± S.D. of at least three experiments. Comparisons among multiple groups were made by analysis of variance. $p < 0.05$ was considered statistically significant. *In vivo*: data

from one wound of a mouse was compared with the other wound on the same mice using paired *t* test.

RESULTS

Micromolar concentrations of H_2O_2 induced VEGF protein expression in human HaCaT as well as primary keratinocytes (Fig. 1, *A–C*). Under conditions of co-existence, the effects of TNFα and H_2O_2 on VEGF induction were additive (Fig. 1*C*). Simultaneous study of multiple angiogenesis-related genes using RNase protection assay indicated that VEGF mRNA is specifically sensitive to H_2O_2 exposure and that the control is at the transcriptional level (Fig. 2*A*). Keratinocytes are not known to have functional VEGF receptors. Our results indicate the absence of Flt receptors in HaCaT (Fig. 2*A*). Several homologues of VEGF, VEGF-A, -B, -C, and -D, have been cloned. Most of the biologically important known functions of VEGF are ascribed to VEGF-A. Less is known about the function and regulation of VEGF-B, -C, and -D, but they do not seem to be regulated by the major pathways that regulate VEGF-A (25, 26). Specific study of the various forms of VEGF showed that all four varieties of VEGF are expressed in HaCaT. VEGF-A is selectively induced by H_2O_2. Among the three splice variants of VEGF-A studied, the 206 form was absent in HaCaT (not shown). Both splice variants of VEGF-A detected in HaCat were induced in response to H_2O_2 treatment (Fig. 2*B*). To characterize the transcriptional control of the VEGF gene by H_2O_2, HaCaT cells were transiently transfected with VEGF promoter-luciferase constructs. This line of investigation was started using a 2.6-kb VEGF promoter fragment (bp −2361 to +298, relative to transcription start site) ligated to a luciferase reporter gene (Fig. 3*A*). Fig. 3*B* shows that H_2O_2 clearly induced luciferase expression driven by the 2.6-kb promoter construct. To define the region of the VEGF promoter responsive to H_2O_2, we utilized a series of 5′ deletions of 2.6-kb promoter vector as demonstrated schematically in Fig. 3*A*. These deletion mutants were then transiently transfected to HaCaT keratinocytes to test the effect of H_2O_2 treatment. H_2O_2 induced reporter activity in the 2.6-, 1.5- as well as 0.35-kb (bp −194 to +157) VEGF promoter constructs. Under these conditions, baseline reporter activity was comparably detected when the above-mentioned three constructs were used (Fig. 3*B*). Interestingly, when the 0.2-kb (bp −50 to +157) construct was used, both baseline as well as H_2O_2-induced reporter activity was completely lost. Similar results were obtained when the 0.07-kb (−50 to +18) construct was used. These results suggest that the sequence from bp −194 to −50 of the VEGF promoter is responsible for the H_2O_2 response. The 144-bp VEGF element (bp −194 to −51) that conferred H_2O_2-mediated transcriptional induction is GC-rich and contains four closely spaced GC boxes (bp −94 to −51) that have been identified to have Sp1 binding function in electrophoretic mobility shift assays (27). Therefore, we sought to test whether these Sp1 binding sites were responsible to confer oxidant sensitivity to the VEGF promoter constructs. To accomplish this goal, a Sp-1 luc reporter construct containing three consensus Sp1 binding sites upstream of the luciferase gene was used. In experiments where HaCaT cells were transiently transfected with the Sp1-luc promoter construct, H_2O_2 indeed induced luciferase expression as shown in Fig. 3*C*. Further evidence to support that Sp1 plays a key role in oxidant-induced VEGF expression was obtained from experiments showing that H_2O_2-induced VEGF

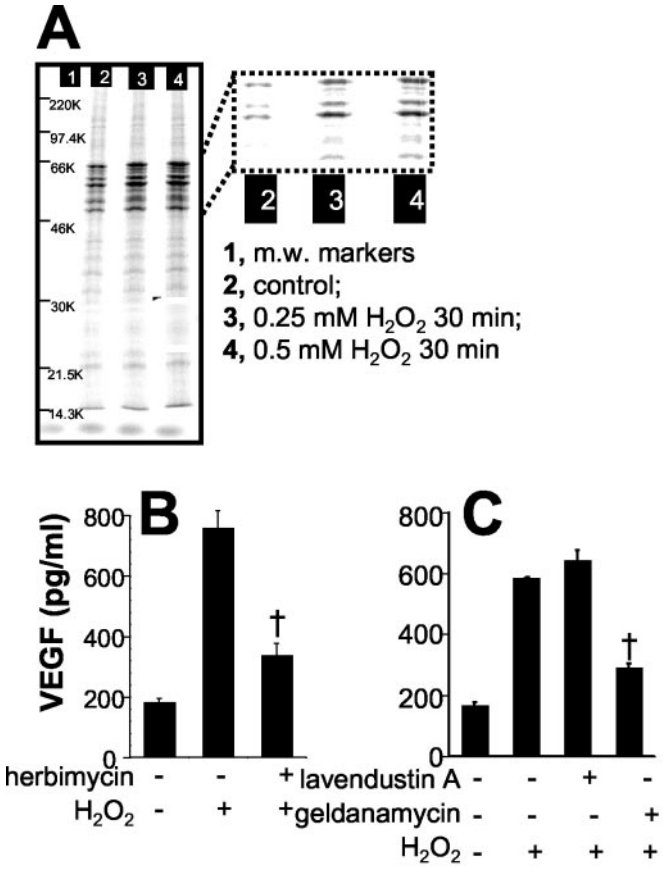

FIG. 4. **Involvement of protein tyrosine phosphorylation in H_2O_2-induced VEGF production.** *A*, ^{35}S-labeled tyrosine phosphorylated proteins were immunoprecipitated from extract of HaCaT cells treated with H_2O_2 for 30 min. ^{35}S-labeled proteins were resolved using SDS-PAGE and subsequently detected using autoradiography. *B* and *C*, cells were treated with either herbimycin A (1 μM), geldanamycin (1 μM; both c-Src kinase inhibitors) or lavendustin A (5 μM; extracellular growth factor receptor tyrosine kinase inhibitor) for 15 min before H_2O_2 treatment. †, $p < 0.001$ when compared with corresponding group not tested with the tyrosine kinase inhibitor.

FIG. 5. **Involvement of NADPH oxidase in inducible VEGF expression.** *A*, Rac1 expression in HaCaT cells transiently transfected with empty plasmid (pEXV) or expression plasmid containing the constitutively active Rac1 gene (pEXVracV12). *B*, Rac1 overexpression increased VEGF expression and markedly potentiated H_2O_2-induced VEGF expression. The NADPH oxidase inhibitor DPI (5 μM) and apocynin (not shown) attenuated inducible VEGF expression. *, $p < 0.05$ compared with pEXV-transfected cells not treated with H_2O_2; †, $p < 0.001$ when compared with the pEXV-transfected group; ‡, $p < 0.001$ lower than the corresponding DPI-untreated group.

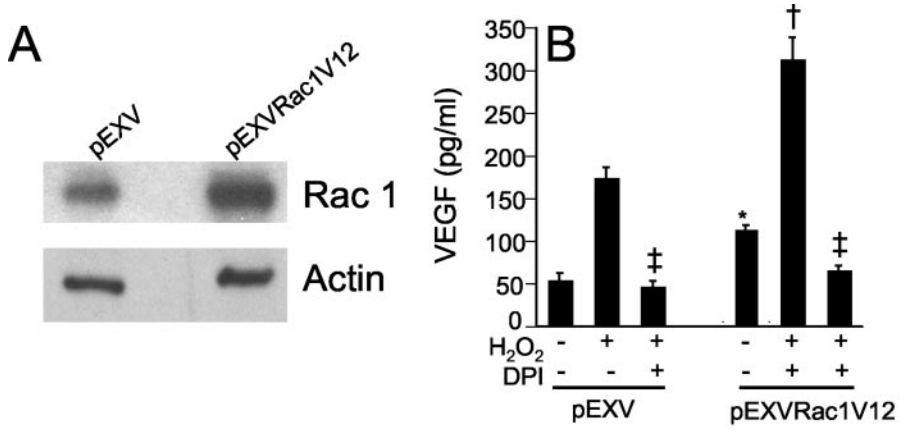

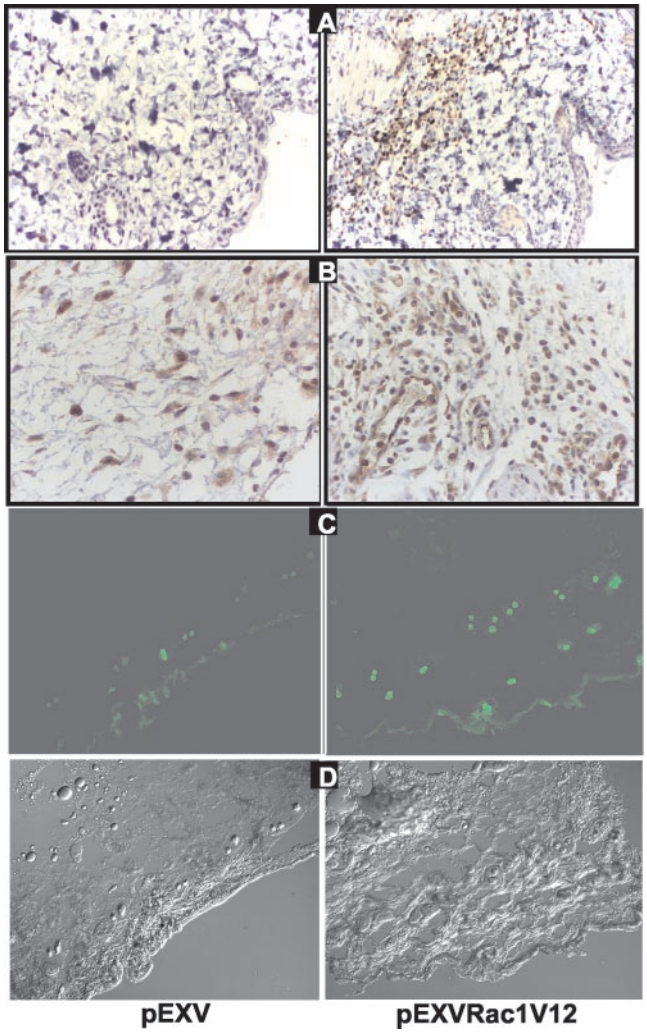

FIG. 6. **Wound edge in response to Rac1 gene transfer.** Rac1 (*A*) and VEGF (*B*) expression on day 3 post-wounding. *C*, Rac1 gene transfer promoted endothelial cell proliferation in FVB/N-TgN-TIE2GFP mice with GFP-tagged endothelial cells. *D*, image of the same frame shown in *C* using differential interference contrast (DIC, Nomarski) optics.

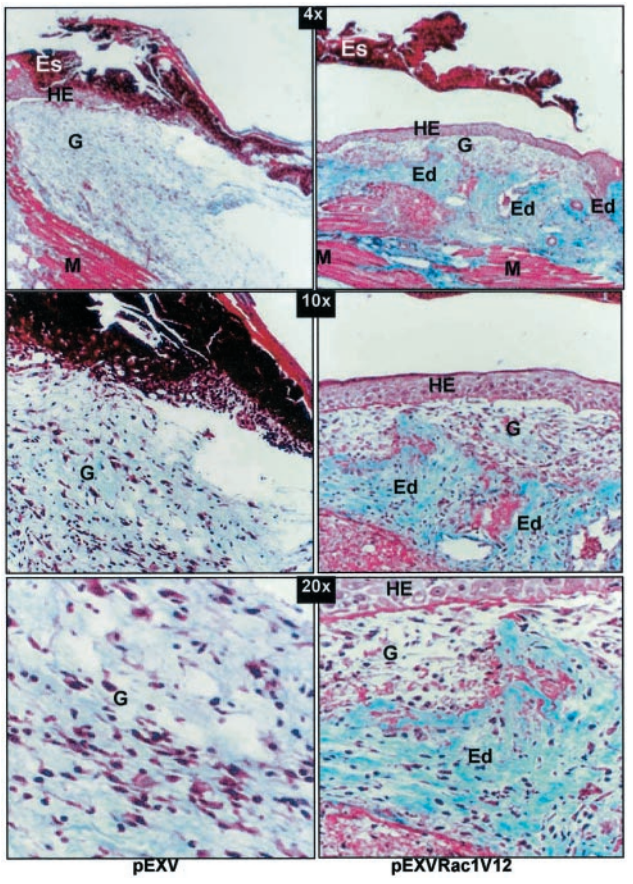

FIG. 7. **Wound edge histology in response to Rac1 gene transfer.** Formalin-fixed paraffin sections from wound edges harvested on post-wounding day 3 were stained using the Masson Trichrome procedure. *Ed*, enhanced deposition of connective tissue (*bluish stain*); *Es*, eschar; *G*, granulation tissue; *HE*, hyperproliferative epithelium; *M*, muscle

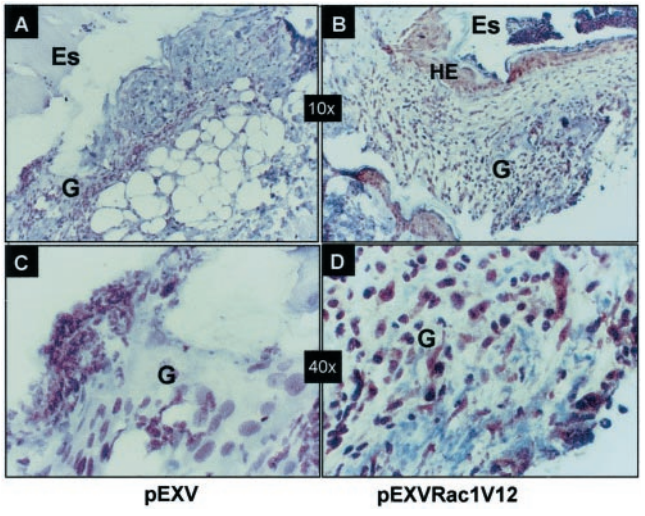

FIG. 8. **Tenascin expression in wound edge in response to Rac1 gene transfer.** Post-wounding day 3 tissue. *Es*, eschar; *G*, granulation tissue; *HE*, hyperproliferative epithelium.

expression is inhibited by the Sp1 transcription inhibitor mithramycin A (Fig. 3*D*).

Hypoxia, a major regulator of inducible VEGF expression, is known to regulate VEGF by a pathway that is characterized by the presence of c-Src kinase upstream and by hypoxia-inducible factor (HIF)-1 downstream (28). As reported above, deletion analysis of VEGF reporter construct revealed that the HIF-1 sites in the VEGF-promoter were not involved in H_2O_2-induced VEGF transactivation. 2-Aminopurine is a serine-threonine kinase inhibitor that specifically blocks certain cellular events including inducibility (29) and DNA binding of HIF-1. Because activation of HIF-1 has been shown to be redox-sensitive we examined the effect of 2-aminopurine on H_2O_2-induced VEGF release (Fig. 3*E*). The observation that 2-aminopurine does not influence H_2O_2-induced VEGF expression is consistent with results reported in Fig. 3*B* indicating that H_2O_2-induced VEGF expression is not mediated by HIF-1 signaling. This observation supports the hypothesis that the downstream regulators of hypoxia and oxidant-induced VEGF expression are different.

Exposure of cells to oxidants such as H_2O_2 is known to induce protein tyrosine phosphorylation primarily by inhibiting SH-rich protein tyrosine phosphatases (3, 18). The concentration of H_2O_2 that induced VEGF expression also induced protein tyrosine phosphorylation. Studies using protein tyrosine kinase inhibitors showed that c-Src kinase inhibitors such as herbimycin and geldanamycin inhibited H_2O_2-induced VEGF expression in HaCaT cells. Receptor protein tyrosine kinase inhibitor lavendustin A did not influence H_2O_2-induced VEGF expression (Fig. 4).

To test the effect of Rac1 overexpression on basal and H_2O_2-

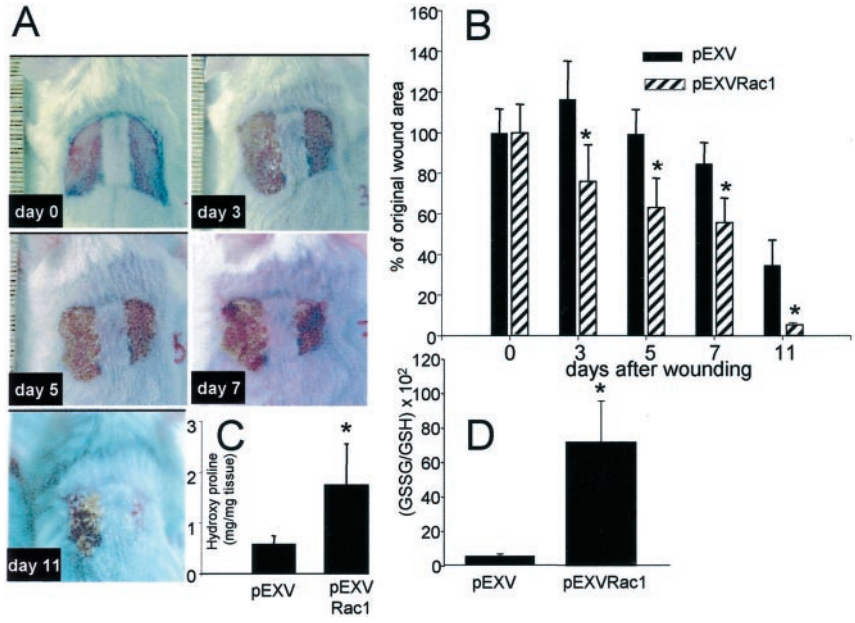

FIG. 9. **Rac1 gene transfer and wound closure.** *A*, the secondary intention wound (8 × 16 mm full-thickness) model (Day 0). Digital images of the left (treated with pEXV) and right (treated with pEXVracV12) side wounds are shown between days 0–11. *B*, wound closure, shown as percentage of area of initial wound determined on the indicated day after wounding. *C*, wound edge hydroxyproline content was measured as an index of collagen deposition. *D*, GSSG/GSH ratio was determined as a marker of oxidation. Mean ± S.D. *, $p < 0.05$ by paired *t* test.

inducible VEGF expression, HaCaT cells were transiently transfected with an empty expression vector pEXV or an active expression vector encoding the constitutively active (rac1V12) Myc epitope-tagged cDNAs of Rac1. Transient transfection of cells with rac1V12 increased Rac1 protein expression as detected by immunoblotting (Fig. 5*A*). Rac1 overexpression clearly increased VEGF expression under resting conditions as well as that induced by H_2O_2 (Fig. 5*B*). The synergistic effect of Rac1 overexpression and H_2O_2 was best observed when a lower concentration of H_2O_2 was used to trigger submaximal VEGF expression. The potentiating effect of Rac1 on inducible VEGF expression was sensitive to DPI as well as apocynin (1–2.5 mM; not shown) suggesting that the observed effect of Rac1 was mediated by NADPH oxidase activity. These results suggest that under resting conditions HaCaT cells abundantly express Rac1. Transfection with rac1V12 further elevated Rac1 protein levels in the cell. Overexpression of Rac1 induced VEGF expression by a NADPH oxidase-dependent mechanism.

To test the effect of Rac1 on wound contraction and closure, each of the two cutaneous wounds was topically treated either with the empty plasmid (pEXV) or with the expression plasmid encoding constitutively active Rac1 (rac1V12) for 4 days postwounding. Rac1 overexpression in response to rac1V12 treatment is shown in Fig. 6*A*. The rac1V12-treated side also showed more prominent VEGF staining as shown in Fig. 6*B*. With the objective to detect endothelial cells we attempted to stain these same histological sections for the detection of CD31. Because of poor quality commercial antibody we were not able to obtain satisfactory staining specific for endothelial cells. To study effect of Rac1 gene therapy on endothelial cell proliferation, similar wounds were placed on the dorsal skin of FVB/N-TgN-TIE2GFP mice. We observed that Rac1 overexpression was associated with a larger number of GFP-tagged endothelial cells in the healing wound (Fig. 6, *C* and *D*).

For a more detailed visualization of the histological architecture of the wound edge tissue, sections were subjected to trichrome staining (Fig. 7). Rac1 gene therapy was associated with a more well defined hyperproliferative epithelial region, higher cell density, enhanced deposition of connective tissue, and improved overall histological organization. Fig. 9*C* provides direct biochemical evidence confirming that Rac1 gene therapy was indeed associated with higher wound edge collagen content as determined by hydroxyproline measurement. Wound healing is associated with a marked increase in the expression of the extracellular matrix glycoprotein tenascin (30). Tenascin expression, a marker of wound repair, was clearly more prominent in wounds subjected to Rac1 gene therapy (Fig. 8). In summary, the histological data indicated that Rac1 might be an important stimulator of various aspects of the repair process, eventually enhancing the wound healing process as a whole (Figs. 7–9).

A representative case where the left wound was treated with pEXV and the right wound was treated with rac1V12 is shown in Fig. 9*A*. Rac1 gene transfer clearly accelerated wound closure, and the effect was clearly seen from day 1 after wounding (Fig. 9*B*). One of the most rapid responses to increased accumulation of oxidants is the prompt oxidation of GSH to GSSG. Rac1-dependent cellular oxidant generation has been demonstrated in several previous studies (10, 12, 13). Fig. 9*D* provides direct evidence attesting that Rac1 gene transfer promoted oxidant generation in the wound edges.

DISCUSSION

Activated phagocytic cells generate ROS as bactericidal agents by a NADPH oxidase-dependent respiratory burst mechanism (1). More recently, non-phagocytic cells have been identified to generate ROS by a NADPH oxidase-dependent system (31). Deficiencies in NADPH oxidase function causes chronic granulomatous disease, a disorder that is associated with wound infection and impaired wound healing (32). Recent studies indicate that ROS may serve as signaling mediators (4). Among the various forms of ROS, H_2O_2 is relatively stable, membrane-permeable, and therefore a good candidate to serve as a cellular messenger (33). We postulated that by virtue of its signal transduction regulatory properties, ROS mediate some of the beneficial effects of oxygen on wound healing. Specifically, we observed that H_2O_2 induces VEGF expression (6, 7). ROS not only support angiogenesis but also stimulate collagen production (34), a key event in wound healing. The wound microenvironment is dynamic involving activity of a number of chemical mediators. Under conditions of co-existence, H_2O_2 and TNFα co-operated to enhance inducible VEGF expression (Fig. 1). Deletion analysis using a series of mutant VEGF promoter constructs revealed that H_2O_2 induced VEGF expression is not mediated by HIF-1. HIF-1 is a major regulator of inducible VEGF expression. Although HIF-1β confers sensitiv-

ity to oxygen (35), our results show that oxidants do not require HIF-1 to induce VEGF expression (Fig. 3). The sequence from bp −194 to −50 of the VEGF promoter was responsible for the H_2O_2 response. The 144-bp VEGF element (bp −194 to −51) that conferred H_2O_2-mediated transcriptional induction is GC-rich and contains four closely spaced GC boxes (bp −94 to −51) that have been identified to have Sp1 binding function in electrophoretic mobility shift assays (27). Direct studies using Sp1 promoter constructs as well as the Sp1 inhibitor mithramycin identified that Sp1 sites in the sequence from bp −194 to −50 of the VEGF promoter are responsible for the H_2O_2 response (Fig. 3). A single major transcription start is known to be located near these Sp1 binding sites in the VEGF gene promoter. Similar to H_2O_2, cytokines such as bFGF, platelet-derived growth factor, and TNFα are known to induce VEGF expression by a mechanism that requires Sp1 but not HIF (36, 37). Transcription control of the inducible VEGF gene by Sp1 is bidirectional. While our results show that Sp1 mediates induction of VEGF expression by oxidant, von Hippel-Lindau tumor suppressor gene-mediated transcriptional repression of VEGF expression is caused by a direct inhibitory action on Sp1 (27).

Catalytically active NADPH oxidase univalently reduces molecular oxygen to generate $O_2^{\cdot-}$, which in turn rapidly dismutates to form H_2O_2. Upon appropriate stimulation, a functional NADPH oxidase is assembled when the cytosolic proteins $p47^{phox}$, $p67^{phox}$, $p40^{phox}$, and the small GTPase Rac (Rac1 or -2) associate with a membrane-localized flavocytochrome (cytochrome b559). The closely related small GTP-binding proteins Rac1, Rac2, and Rac3 are part of a larger Rho subfamily of Ras proteins. Rac1 controls actin redistribution to membrane ruffles in fibroblasts and other cell types, as well as the activation of the NADPH oxidase in both phagocytes as well as non-phagocytic cells (11, 14, 38). Direct evidence supporting a mitogenic function of oxidants generated by Rac1 has been reported (10, 13). Although under conditions such as reoxygenation injury, Rac1-dependent oxidant production may prove to be deleterious (12), we sought to utilize the oxidant-generating ability of Rac1 to accelerate wound healing. *In vitro*, Rac1 overexpression increased VEGF expression and worked synergistically with H_2O_2 to enhance VEGF expression in a NADPH oxidase-dependent manner. *In vivo*, Rac1 overexpression was associated with more prominent expression of VEGF and proliferation of endothelial cells. Study of the spatial control of growth factor-induced Rac activation revealed that Rac1 activation is associated with activation at the leading edge of motile cells (39). Remodeling of the extracellular matrix and consequent alterations of integrin-mediated adhesion and cytoarchitecture are central to wound healing. It has been observed that activation of Rac1 may lead to altered gene regulation and alterations in cellular morphogenesis, migration, and invasion (40). Consistent with these findings, we observed that Rac1 gene transfer clearly facilitated murine excisional dermal wound closure and tissue remodeling. These findings are in line with the proposed central role of Rac1 in regulating cellular morphogenesis and migration (40).

Taken together, the results of this study provide firm support to the claim that wound healing is subject to redox control. It is established that μM oxidant induces VEGF expression and that oxidant-induced VEGF expression is independent of HIF-1 and dependent on Sp1. Using the Rac1 gene transfer approach it is documented that strategies to promote oxidant production in the wound microenvironment may promote wound healing.

Acknowledgments—Technical assistance of J. Vider and M. Venojarvi is gratefully acknowledged. The Laboratory of Molecular Medicine is the research division of the Center for Minimally Invasive Surgery.

REFERENCES

1. Babior, B. M., Kipnes, R. S., and Curnutte, J. T. (1973) *J. Clin. Invest.* **52,** 741–744
2. Sen, C. K., Sies, H., and Baeuerle, P. A. (eds) (2000) *Antioxidant and Redox Regulation of Genes*, Academic Press, San Diego
3. Sen, C. K., and Packer, L. (1996) *FASEB J.* **10,** 709–720
4. Sen, C. K. (2000) *Curr. Top. Cell. Reg.* **36,** 1–30
5. Sen, C. K. (1998) *Biochem. Pharmacol.* **55,** 1747–1758
6. Sen, C. K., Khanna, S., Venojarvi, M., Trikha, P., Ellison, E. C., Hunt, T. K., and Roy, S. (2002) *Am. J. Physiol.* **282,** H1821–H1827
7. Khanna, S., Roy, S., Bagchi, D., Bagchi, M., and Sen, C. K. (2001) *Free Radic. Biol. Med.* **31,** 38–42
8. Cho, M., Hunt, T. K., and Hussain, M. Z. (2001) *Am. J. Physiol.* **280,** H2357–H2363
9. Heyworth, P. G., Knaus, U. G., Settleman, J., Curnutte, J. T., and Bokoch, G. M. (1993) *Mol. Biol. Cell* **4,** 1217–1223
10. Irani, K., Xia, Y., Zweier, J. L., Sollott, S. J., Der, C. J., Fearon, E. R., Sundaresan, M., Finkel, T., and Goldschmidt-Clermont, P. J. (1997) *Science* **275,** 1649–1652
11. Sundaresan, M., Yu, Z. X., Ferrans, V. J., Sulciner, D. J., Gutkind, J. S., Irani, K., Goldschmidt-Clermont, P. J., and Finkel, T. (1996) *Biochem. J.* **318** 379–382
12. Kim, K. S., Takeda, K., Sethi, R., Pracyk, J. B., Tanaka, K., Zhou, Y. F., Yu, Z. X., Ferrans, V. J., Bruder, J. T., Kovesdi, I., Irani, K., Goldschmidt-Clermont, P., and Finkel, T. (1998) *J. Clin. Invest.* **101,** 1821–1826
13. Joneson, T., and Bar-Sagi, D. (1998) *J. Biol. Chem.* **273,** 17991–17994
14. Moldovan, L., Irani, K., Moldovan, N. I., Finkel, T., and Goldschmidt-Clermont, P. J. (1999) *Antiox. Redox Signal.* **1,** 29–43
15. Slansky, J. E., Li, Y., Kaelin, W. G., and Farnham, P. J. (1993) *Mol. Cell. Biol.* **13,** 1610–1618
16. Mukhopadhyay, D., Tsiokas, L., and Sukhatme, V. P. (1995) *Cancer Res.* **55,** 6161–6165
17. Boukamp, P., Petrussevska, R. T., Breitkreutz, D., Hornung, J., Markham, A., and Fusenig, N. E. (1988) *J. Cell Biol.* **106,** 761–771
18. Sen, C. K., Khanna, S., Roy, S., and Packer, L. (2000) *J. Biol. Chem.* **275,** 13049–13055
19. Sen, C. K., Roy, S., Khanna, S., and Packer, L. (1999) *Meth. Enzymol.* **299,** 239–246
20. Roy, S., Venojarvi, M., Khanna, S., and Sen, C. K. (2002) *Meth. Enzymol.* **352,** 326–332
21. Yu, W. H., Kashani-Sabet, M., Liggitt, D., Moore, D., Heath, T. D., and Debs, R. J. (1999) *J. Invest. Dermatol.* **112,** 370–375
22. Sambrook, J., Fritsch, E. F., and Maniatis, T. (1989) *Molecular Cloning: A Laboratory Manual*, Cold Spring Harbor Laboratory Press, Cold Spring Harbor, New York
23. Brown, S., Worsfold, M., and Sharp, C. (2001) *BioTechniques* **30,** 38–40
24. Bancroft, J. D., and Stevens, A. (eds) (1996) *Theory and Practice of Histological Techniques*, Churchill Livingstone, Edinburgh, Scotland
25. Carmeliet, P., and Collen, D. (1999) *Curr. Top. Microbiol. Immunol.* **237,** 133–158
26. Eriksson, U., and Alitalo, K. (1999) *Curr. Top. Microbiol. Immunol.* **237,** 41–57
27. Mukhopadhyay, D., Knebelmann, B., Cohen, H. T., Ananth, S., and Sukhatme, V. P. (1997) *Mol. Cell. Biol.* **17,** 5629–5639
28. Mukhopadhyay, D., Tsiokas, L., Zhou, X. M., Foster, D., Brugge, J. S., and Sukhatme, V. P. (1995) *Nature* **375,** 577–581
29. Wang, G. L., and Semenza, G. L. (1993) *J. Biol. Chem.* **268,** 21513–21518
30. Latijnhouwers, M. A., Bergers, M., Van Bergen, B. H., Spruijt, K. I., Andriessen, M. P., and Schalkwijk, J. (1996) *J. Path.* **178,** 30–35
31. Suh, Y. A., Arnold, R. S., Lassegue, B., Shi, J., Xu, X., Sorescu, D., Chung, A. B., Griendling, K. K., and Lambeth, J. D. (1999) *Nature* **401,** 79–82
32. Eckert, J. W., Abramson, S. L., Starke, J., and Brandt, M. L. (1995) *Am. J. Surg.* **169,** 320–323
33. Baeuerle, P. A., Rupec, R. A., and Pahl, H. L. (1996) *Path. Biol.* (*Paris*) **44,** 29–35
34. Chandrakasan, G., and Bhatnagar, R. S. (1991) *Cell. Mol. Biol.* **37,** 751–755
35. Semenza, G. L. (2000) *Cancer Met. Rev.* **19**, 59–65
36. Ryuto, M., Ono, M., Izumi, H., Yoshida, S., Weich, H. A., Kohno, K., and Kuwano, M. (1996) *J. Biol. Chem.* **271,** 28220–28228
37. Finkenzeller, G., Sparacio, A., Technau, A., Marme, D., and Siemeister, G. (1997) *Oncogene* **15,** 669–676
38. Cool, R. H., Merten, E., Theiss, C., and Acker, H. (1998) *Biochem. J.* **332,** 5–8
39. Kraynov, V. S., Chamberlain, C., Bokoch, G. M., Schwartz, M. A., Slabaugh, S., and Hahn, K. M. (2000) *Science* **290,** 333–337
40. Kheradmand, F., Werner, E., Tremble, P., Symons, M., and Werb, Z. (1998) *Science* **280,** 898–902
41. Liu, Y., Cox, S. R., Morita, T., and Kourembanas, S. (1995) *Cir. Res.* **77,** 638–643
42. Tischer, E., Mitchell, R., Hartman, T., Silva, M., Gospodarowicz, D., Fiddes, J. C., and Abraham, J. A. (1991) *J. Biol. Chem.* **266,** 11947–11954

Oxidant-induced Vascular Endothelial Growth Factor Expression in Human Keratinocytes and Cutaneous Wound Healing

Chandan K. Sen, Savita Khanna, Bernard M. Babior, Thomas K. Hunt, E. Christopher Ellison and Sashwati Roy

J. Biol. Chem. 2002, 277:33284-33290.
doi: 10.1074/jbc.M203391200 originally published online June 14, 2002
